

Beating quantum limits in optomechanical sensor by cavity detuning

O. Arcizet, T. Briant, A. Heidmann, and M. Pinard

*Laboratoire Kastler Brossel, Case 74, 4 place Jussieu, F75252 Paris Cedex 05, France**

(Dated: January 30, 2006)

We study the quantum limits in an optomechanical sensor based on a detuned high-finesse cavity with a movable mirror. We show that the radiation pressure exerted on the mirror by the light in the detuned cavity induces a modification of the mirror dynamics and makes the mirror motion sensitive to the signal. This leads to an amplification of the signal by the mirror dynamics, and to an improvement of the sensor sensitivity beyond the standard quantum limit, up to an ultimate quantum limit only related to the mechanical dissipation of the mirror. This improvement is somewhat similar to the one predicted in detuned signal-recycled gravitational-waves interferometers, and makes a high-finesse cavity a model system to test these quantum effects.

PACS numbers: 42.50.Lc, 03.65.Ta, 04.80.Nn

I. INTRODUCTION

Quantum noise of light is known to induce fundamental limits in very sensitive optical measurements. As an example, the future generations of gravitational-wave interferometers [1, 2, 3] will most probably be confronted to quantum effects of radiation pressure. A gravitational wave induces a differential variation of the optical paths in the two arms of a Michelson interferometer. The detection of the phase difference between the two paths is ultimately limited by two quantum noise sources: the phase fluctuations of the incident laser beam and the radiation pressure effects which induce unwanted mirror displacements in the interferometer. A compromise between these noises leads to the so-called standard quantum limit for the sensitivity of the measurement [4, 5, 6].

Number of quantum noise reduction schemes have been proposed which rely on the injection of squeezed states of light in the interferometer [7, 8, 9], or on the quantum correlations induced by radiation pressure between phase and intensity fluctuations in the interferometer [10]. The possibility to implement these techniques in real interferometers gave rise to new methods such as the quantum locking of mirrors [11] or the detuning of the signal recycling cavity [12, 13].

It seems important to find simple systems where similar quantum effects can be produced and characterized in order to test these effects in tabletop experiments. From this point of view, high-finesse optical cavities with movable mirrors have interesting potentialities since they exhibit similar quantum limits. Several schemes involving such cavities have been proposed either to create non-classical states of both the radiation field [14, 15] and of the mirror motion [16, 17, 18], or to perform quantum nondemolition measurements [19]. Recent progress in low-noise laser sources and low-loss mirrors have made

the field experimentally accessible [20, 21, 22].

We study in this paper the quantum effects in a detuned cavity and the possibility to beat the standard quantum limit. As for signal-recycled interferometers [23], the detuning of the cavity induces a modification of the mechanical dynamics of the mirror, known as optical spring. This effect may improve the sensitivity beyond the standard quantum limit since it changes the mechanical rigidity of the mirror without any additional noise [24, 25]. The optical spring has already been observed in a Fabry-Perot cavity [26], and studied both theoretically [27] and experimentally [28] for its role in parametric instabilities.

We perform a full quantum treatment of a detuned cavity with a movable mirror. We show that the sensitivity of the measurement of a cavity length variation can be made better than the standard quantum limit. From a careful analysis of the mirror dynamics, we find that it is not only attributed to the optical spring, but also to the fact that the mirror becomes sensitive to the signal through the radiation pressure exerted on the mirror. We show that the mirror motion can amplify the signal, thus increasing the sensitivity up to an ultimate quantum limit only related to the dissipation mechanisms of the mechanical motion [5]. We finally study the influence of a finite cavity bandwidth and obtain dual sensitivity peaks similar to the ones obtained for detuned signal-recycled interferometers [12].

II. OPTOMECHANICAL COUPLING IN A DETUNED CAVITY

We consider the single-port cavity shown in Fig. 1 with a partially transmitting front mirror and a totally reflecting end mirror. A probe laser beam is sent in the cavity and the phase of the reflected field is monitored by a homodyne detection. We consider in the following the motion of a single mirror assuming the front mirror is fixed, and we note X_m the displacement of the movable end mirror. We study the response of the system to a signal described as a variation X_{sig} of the cavity

*Unité mixte de recherche du Centre National de la Recherche Scientifique, de l'École Normale Supérieure et de l'Université Pierre et Marie Curie; URL: www.spectro.jussieu.fr/Mesure

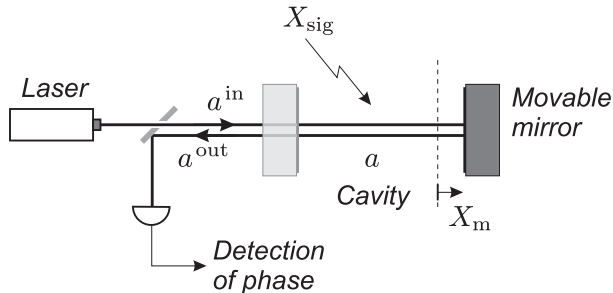


FIG. 1: A length variation X_{sig} is measured by a single-ended Fabry-Perot cavity through the phase shift induced on the reflected field a^{out} . Radiation pressure effects are taken into account via the displacement X_m of the movable end mirror.

length. It can either be a physical variation of the cavity length due for example to an external force applied on the movable mirror, or an apparent variation such as the one produced by a gravitational wave in a gravitational-wave interferometer. The time-dependent cavity length L is then given by

$$L(t) = L_0 + X_m(t) + X_{\text{sig}}(t), \quad (1)$$

where L_0 is the cavity length without signal and for a mirror at rest.

For a nearly resonant high-finesse cavity, the intracavity field mode described by the annihilation and creation operators $a(t)$ and $a^\dagger(t)$ is related to the input and output fields $a^{\text{in}}(t)$ and $a^{\text{out}}(t)$ by

$$\tau \frac{da(t)}{dt} = -[\gamma - i\psi(t)]a(t) + \sqrt{2\gamma}a^{\text{in}}(t), \quad (2)$$

$$a^{\text{out}}(t) = -a^{\text{in}}(t) + \sqrt{2\gamma}a(t), \quad (3)$$

where γ is the damping rate of the cavity assumed to be small compared to 1, τ is the cavity round trip time, and $\psi(t)$ is the time-dependent detuning of the cavity related to the cavity length by

$$\psi(t) \equiv 2kL(t)[2\pi], \quad (4)$$

where k is the field wavevector.

The intracavity field induces a radiation pressure force F_{rad} on the mirror which is proportional to the field intensity,

$$F_{\text{rad}}(t) = 2\hbar k I(t), \quad (5)$$

where the intracavity intensity $I = |a|^2$ is normalized as a photon flux. In the framework of linear response theory [29], the Fourier transform $X_m[\Omega]$ of the mirror displacement at frequency Ω linearly depends on the applied force $F[\Omega]$,

$$X_m[\Omega] = \chi[\Omega] F[\Omega], \quad (6)$$

where $\chi[\Omega]$ is the mechanical susceptibility of the mirror. Assuming that the mirror motion can be described as

the one of a single harmonic oscillator with a resonance frequency Ω_M , a mass M , and a damping rate Γ , the susceptibility has the simple form

$$\chi[\Omega] = \frac{1}{M(\Omega_M^2 - \Omega^2 - i\Gamma\Omega)}. \quad (7)$$

The steady state is obtained by cancelling the time derivative in (2). One gets the steady states \bar{a} and \bar{a}^{out} of the intracavity and output fields as a function of the incident mean field \bar{a}^{in} and the mean detuning $\bar{\psi}$ of the cavity,

$$\bar{a} = \frac{\sqrt{2\gamma}}{\gamma - i\bar{\psi}} \bar{a}^{\text{in}} = \frac{\sqrt{2\gamma}}{\gamma + i\bar{\psi}} \bar{a}^{\text{out}}. \quad (8)$$

As expected for a lossless cavity, the outgoing mean intensity $|\bar{a}^{\text{out}}|^2$ is equal to the incident one $|\bar{a}^{\text{in}}|^2$. For a non-zero detuning $\bar{\psi}$, the mean fields \bar{a}^{in} , \bar{a} , and \bar{a}^{out} have different phases. We choose by convention the arbitrary global phase of the fields in such a way that the intracavity field \bar{a} is real. The phases θ^{in} and θ^{out} of the input and output mean fields are then given by

$$e^{-i\theta^{\text{in}}} = \frac{\gamma - i\bar{\psi}}{\sqrt{\gamma^2 + \bar{\psi}^2}}, \quad e^{-i\theta^{\text{out}}} = \frac{\gamma + i\bar{\psi}}{\sqrt{\gamma^2 + \bar{\psi}^2}}. \quad (9)$$

According to eqs. (1) to (6), the mean detuning $\bar{\psi}$ depends on the intracavity intensity through the mirror recoil induced by the intracavity radiation pressure,

$$\bar{\psi} = \psi_0 + \hbar\kappa^2\chi[0], \quad (10)$$

where $\psi_0 \equiv 2kL_0[2\pi]$ is the detuning without light and $\kappa = 2k|\bar{a}|$. The coupled equations (8) and (10) give a third order relation between \bar{a} and $\bar{\psi}$ which leads to the well known bistable behavior of a cavity with a movable mirror [30]. The stability condition of the system can be written as

$$\gamma^2 + \bar{\psi}^2 + 2\hbar\kappa^2\chi[0]\bar{\psi} > 0, \quad (11)$$

III. MIRROR DYNAMICS

We derive in this section the basic input-output relations for the fluctuations and we study the modification of the mirror dynamics induced by the radiation pressure in the cavity. We will show that the mechanical response of the mirror to an external force is modified by the optomechanical coupling with the light. It can be described by an effective mechanical susceptibility similar to the one obtained with an active control of the mirror by a feedback loop [21, 31, 32].

The linearization of the Fourier transform of eq. (2) around the mean state gives the intracavity field $a[\Omega]$, at a given frequency Ω , as a function of the incident field

fluctuations a^{in} and the cavity length variations X_m and X_{sig} ,

$$(\gamma - i\bar{\psi} - i\Omega\tau) a[\Omega] = \sqrt{2\gamma} a^{\text{in}}[\Omega] + i\kappa X_m[\Omega] + i\kappa X_{\text{sig}}[\Omega]. \quad (12)$$

According to eq. (5), the radiation pressure $F_{\text{rad}}[\Omega]$ depends on the intensity fluctuations of the intracavity field at frequency Ω . From eq. (12) it can be written as the sum of three forces,

$$F_{\text{rad}}^{(\text{in})}[\Omega] = \hbar\kappa \sqrt{\frac{2\gamma}{\gamma^2 + \bar{\psi}^2}} \left(\frac{\gamma^2 + \bar{\psi}^2 - i\gamma\Omega\tau}{\Delta} p^{\text{in}}[\Omega] - \frac{i\bar{\psi}\Omega\tau}{\Delta} q^{\text{in}}[\Omega] \right), \quad (13)$$

$$F_{\text{rad}}^{(\text{m})}[\Omega] = -2\hbar\kappa^2 \frac{\bar{\psi}}{\Delta} X_m[\Omega], \quad (14)$$

$$F_{\text{rad}}^{(\text{sig})}[\Omega] = -2\hbar\kappa^2 \frac{\bar{\psi}}{\Delta} X_{\text{sig}}[\Omega], \quad (15)$$

where $\Delta = (\gamma - i\Omega\tau)^2 + \bar{\psi}^2$ and the operators $p^{\text{in}}[\Omega]$ and $q^{\text{in}}[\Omega]$ correspond to the amplitude and phase quadratures of the incident field, respectively,

$$p^{\text{in}}[\Omega] = e^{i\theta^{\text{in}}} a^{\text{in}}[\Omega] + e^{-i\theta^{\text{in}}} a^{\text{in}\dagger}[\Omega], \quad (16)$$

$$q^{\text{in}}[\Omega] = -ie^{i\theta^{\text{in}}} a^{\text{in}}[\Omega] + ie^{-i\theta^{\text{in}}} a^{\text{in}\dagger}[\Omega], \quad (17)$$

(same definitions hold for the intracavity quadratures with an angle $\theta = 0$ and for the reflected ones with the angle θ^{out}). The first force $F_{\text{rad}}^{(\text{in})}$ represents the radiation pressure induced by the quantum fluctuations of the incident field. It is the usual force obtained in the case of a resonant cavity, which is responsible for the generation of squeezing in a cavity with a movable mirror [14]. Since it induces a displacement of the mirror proportional to the field fluctuations, it is also responsible for the standard quantum limits in interferometric measurements [4, 5, 6]. For a resonant cavity ($\bar{\psi} = 0$), this force only depends on the incident intensity fluctuations p^{in} filtered by the cavity bandwidth $\Omega_{\text{cav}} = \gamma/\tau$.

The two other forces $F_{\text{rad}}^{(\text{m})}$ and $F_{\text{rad}}^{(\text{sig})}$ only exist when the cavity is detuned ($\bar{\psi} \neq 0$). In that case the working point of the cavity is on one side of the Airy peak. According to eqs. (4) and (8), the intracavity intensity depends on the cavity length variations with a slope

$$\frac{d\bar{I}}{dX} = -2\kappa \frac{\bar{\psi}}{\gamma^2 + \bar{\psi}^2} \bar{a}. \quad (18)$$

Any length variation changes the intracavity intensity and induces a variation of the radiation pressure exerted on the mirror. This variation corresponds to the forces $F_{\text{rad}}^{(\text{m})}$ and $F_{\text{rad}}^{(\text{sig})}$ which are actually proportional to the slope (18) of the Airy peak,

$$F_{\text{rad}}^{(j)}[\Omega] = 2\hbar\kappa \frac{\gamma^2 + \bar{\psi}^2}{\Delta} \frac{d\bar{I}}{dX} X_j[\Omega], \quad (19)$$

where $j = (\text{m}, \text{sig})$. The first fraction in (19) is a low-pass filter associated with the cavity storage time. The sign of the forces depends on the sign of the slope (18). Depending on the sign of $\bar{\psi}$, the force $F_{\text{rad}}^{(\text{m})}$ is either a repulsive or an attractive force, and the force $F_{\text{rad}}^{(\text{sig})}$ induces a mirror displacement which may either amplify or compensate the signal X_{sig} . We will see in the next section that this signal amplification by the mirror motion is at the basis of the sensitivity improvement obtained with a detuned cavity.

The force $F_{\text{rad}}^{(\text{m})}$ is proportional to the mirror displacement X_m . Its effect is to change the mechanical response of the mirror to an external force which is now given by eq. (6) with an effective susceptibility χ_{eff} related to the free susceptibility χ by

$$\chi_{\text{eff}}^{-1}[\Omega] = \chi^{-1}[\Omega] + 2\hbar\kappa^2 \frac{\bar{\psi}}{\Delta}. \quad (20)$$

If the frequencies Ω and Ω_M are much smaller than the cavity bandwidth Ω_{cav} , the additional term in (20) is real. As a consequence, its effect is to change the spring constant of the mechanical motion [24], that is to shift the resonance frequency Ω_M of the oscillator [eq. (7)], either to low or high frequencies depending on the sign of $\bar{\psi}$. If the frequencies Ω and Ω_M are of the order of Ω_{cav} , the additional term in (20) becomes complex and also changes the imaginary part of the susceptibility. If we consider a mirror with a high quality factor ($\Gamma \ll \Omega_M$), the mechanical response (20) can still be considered as Lorentzian with an effective damping Γ_{eff} given by

$$\Gamma_{\text{eff}} = \Gamma - \frac{4\hbar\kappa^2}{M\Omega_{\text{cav}}} \frac{\gamma^2 \bar{\psi}}{|\Delta|^2}, \quad (21)$$

where the denominator Δ is estimated at frequency Ω_M . The mechanical resonance is widened or narrowed depending on the sign of $\bar{\psi}$.

The coupling with the intracavity field thus changes the dynamics of the mirror, both via its spring constant and its damping. The effect is somewhat similar to the one obtained with an external feedback control. In both cases it is for example possible to carry out a cold damping mechanism which increases the damping without adding extra thermal fluctuations, thus leading to a reduction of the effective temperature of the mirror [21, 33]. In this paper we will use these effects in another way, in order to amplify the response of the mirror to an external force. Together with the sensitivity of the mirror motion to the signal via the force $F_{\text{rad}}^{(\text{sig})}$, this will allow us to greatly amplify the sensitivity of the cavity to the signal.

Let us note that the modification of the dynamics can lead to an instability where the mirror enters a self-oscillating regime. The dynamic stability condition is usually given by the Ruth-Hurwitz criterium applied to the determinant of the linear relations between the field and the mirror position [14, 34]. It is actually equivalent to the condition that the mirror motion has to be

characterized by a positive damping in order to have a non-divergent motion,

$$\Gamma_{\text{eff}} > 0. \quad (22)$$

IV. SENSITIVITY OF THE MEASUREMENT

We now determine the sensitivity of the measurement and how it is modified by the cavity detuning. We consider for simplicity that the low-pass filtering by the cavity can be neglected, that is all frequencies of interest (Ω , Ω_M) are much smaller than Ω_{cav} . This assumption will be relaxed in section VIII.

The measurement is done by monitoring the phase quadrature q^{out} of the field reflected by the cavity, as shown in Fig. 1. The linearized input-output relations for the field are deduced from eqs. (3) and (12),

$$p^{\text{out}}[\Omega] = p^{\text{in}}[\Omega], \quad (23)$$

$$q^{\text{out}}[\Omega] = q^{\text{in}}[\Omega] + 2\xi (X_m[\Omega] + X_{\text{sig}}[\Omega]), \quad (24)$$

where the optomechanical coupling parameter ξ is given by

$$\xi = \sqrt{\frac{2\gamma}{\gamma^2 + \bar{\psi}^2}} \kappa = 2k \frac{2\gamma}{\gamma^2 + \bar{\psi}^2} |\bar{a}^{\text{in}}|. \quad (25)$$

The working point of the cavity will be defined in the following by the two independent parameters $\bar{\psi}$ and ξ . Other parameters such as the incident and intracavity intensities can be deduced from eqs. (8) and (25).

Equations (23) and (24) show that as long as we consider the quasi-static regime $\Omega \ll \Omega_{\text{cav}}$, the input-output relations are similar for a resonant and a detuned cavity. Due to the preservation of the photon flux in a lossless single-ended cavity, the reflected amplitude fluctuations are equal to the incident ones and only the reflected phase quadrature is sensitive to the variation $X_m + X_{\text{sig}}$ of the cavity length. This variation is superimposed to the incident phase noise q^{in} .

The mirror is submitted to the radiation pressure of the intracavity field. As shown in the previous section, the response to the forces $F_{\text{rad}}^{(\text{in})}$ and $F_{\text{rad}}^{(\text{sig})}$ [eqs. (13) and (15)] is characterized by the effective mechanical susceptibility χ_{eff} [eq. (20)]. In the limit $\Omega \ll \Omega_{\text{cav}}$, this susceptibility and the resulting motion are given by

$$\chi_{\text{eff}}^{-1}[\Omega] = \chi^{-1}[\Omega] + \hbar\xi^2 \frac{\bar{\psi}}{\gamma}, \quad (26)$$

$$X_m[\Omega] = \chi_{\text{eff}}[\Omega] \left(\hbar\xi p^{\text{in}}[\Omega] - \hbar\xi^2 \frac{\bar{\psi}}{\gamma} X_{\text{sig}}[\Omega] \right). \quad (27)$$

The mirror motion reproduces the signal X_{sig} with a dynamics characterized by the effective susceptibility χ_{eff} . Depending on the sign of $\bar{\psi}\chi_{\text{eff}}[\Omega]$, the mirror displacement is in phase or out of phase with the signal, thus leading to an amplification or a reduction of the signal

in the output phase quadrature. This quadrature is obtained from eqs. (24) and (27),

$$q^{\text{out}}[\Omega] = q^{\text{in}}[\Omega] + 2\hbar\xi^2 \chi_{\text{eff}}[\Omega] p^{\text{in}}[\Omega] + 2\xi \frac{\chi_{\text{eff}}[\Omega]}{\chi[\Omega]} X_{\text{sig}}[\Omega]. \quad (28)$$

The signal X_{sig} is amplified by the coupling parameter ξ and by the dynamics of the mirror χ_{eff}/χ [last term in (28)]. The signal is superimposed to two noises respectively proportional to the phase and amplitude incident fluctuations [first terms in (28)]. These noises are nothing but the usual phase noise and radiation pressure noise in interferometric measurements.

It is instructive to compare the cases of detuned and resonant cavities. For a resonant cavity, there is no modification of the mechanical susceptibility ($\chi_{\text{eff}} = \chi$) and the mirror motion does not depend on the signal. The output quadrature is simply obtained from eq. (28) by replacing χ_{eff} by χ . There is no amplification of the signal and the minimum noise corresponds to the standard quantum limit which is reached when both the phase and radiation pressure noises are of the same order, that is $\hbar\xi^2 |\chi| \approx 1$.

For a detuned cavity, the signal is amplified by the ratio $|\chi_{\text{eff}}/\chi|$, and the radiation pressure noise is also increased by the same factor [second term in eq. (28)]. As long as we are only concerned by the noises, the system is thus equivalent to a resonant cavity with a mirror having an effective susceptibility χ_{eff} . Due to the signal amplification, this is no longer true if we are looking at the signal to noise ratio. The sensitivity of the measurement can be increased beyond the standard quantum limit by choosing the optomechanical parameters ξ and $\bar{\psi}$ in such a way that the signal is amplified ($|\chi_{\text{eff}}| > |\chi|$), whereas the quantum noises are still at the standard quantum limit, that is $\hbar\xi^2 |\chi_{\text{eff}}| \approx 1$.

To derive a more precise evaluation of the sensitivity improvement, we define an estimator \hat{X}_{sig} of the signal, equal to the measured quadrature q^{out} normalized as the length variation X_{sig} ,

$$\hat{X}_{\text{sig}}[\Omega] = \frac{1}{2\xi} \frac{\chi[\Omega]}{\chi_{\text{eff}}[\Omega]} q^{\text{out}}[\Omega]. \quad (29)$$

From eq. (28), this estimator appears as the sum of the signal X_{sig} and two equivalent input noises proportional to the incident fluctuations q^{in} and p^{in} . The sensitivity of the measurement is limited by the spectrum $S_{\text{sig}}[\Omega]$ of these noises. For a coherent incident beam, the quantum fluctuations of the two incident quadratures p^{in} and q^{in} are two independent white noises with a unity spectrum ($S_p^{\text{in}}[\Omega] = S_q^{\text{in}}[\Omega] = 1$). The equivalent noise spectrum $S_{\text{sig}}[\Omega]$ is then given by

$$S_{\text{sig}}[\Omega] = \hbar |\chi[\Omega]| \left| \frac{\chi[\Omega]}{\chi_{\text{eff}}[\Omega]} \right| \frac{\zeta[\Omega] + 1/\zeta[\Omega]}{2}, \quad (30)$$

where the dimensionless parameter ζ is defined as

$$\zeta[\Omega] = 2\hbar\xi^2 |\chi_{\text{eff}}[\Omega]|. \quad (31)$$

The last fraction in eq. (30) is always greater than 1 and reaches its minimum for $\zeta[\Omega] = 1$. In that case, the phase and radiation pressure noises are equal and their sum is minimum. For a resonant cavity, this corresponds to the standard quantum limit which is reached at a given frequency Ω for the following value $\xi_{\text{SQL}}[\Omega]$ of the optomechanical parameter, and corresponds to a minimum noise level $S_{\text{sig}}^{\text{SQL}}[\Omega]$ given by

$$\xi_{\text{SQL}}[\Omega] = \frac{1}{\sqrt{2\hbar} |\chi[\Omega]|}, \quad (32)$$

$$S_{\text{sig}}^{\text{SQL}}[\Omega] = \hbar |\chi[\Omega]|. \quad (33)$$

It is clear from eq. (30) that the standard quantum limit is not a fundamental limit. It is possible to go beyond this limit with a detuned cavity, by choosing the optomechanical parameters so that $\zeta[\Omega] \simeq 1$ and $|\chi_{\text{eff}}[\Omega]| > |\chi[\Omega]|$. The sensitivity is then increased by the amplification factor $|\chi_{\text{eff}}[\Omega]/\chi[\Omega]|$ given by [see eq. (26)],

$$|\chi_{\text{eff}}[\Omega]/\chi[\Omega]| = \left| 1 + \hbar \xi^2 \frac{\bar{\psi}}{\gamma} \chi[\Omega] \right|^{-1}. \quad (34)$$

Note that the term inside the absolute value, taken at frequency $\Omega = 0$, exactly corresponds to the stability condition of the bistable behavior [eq. (11)]. This term is strictly positive in the stable domain, thus preventing the amplification factor to diverge. We study in the next sections the sensitivity improvement in two particular cases of experimental interest, corresponding to a frequency Ω either below or beyond the mechanical resonance frequency Ω_M .

V. SENSITIVITY IMPROVEMENT AT LOW FREQUENCY

We first consider the sensitivity improvement at frequency lower than the mechanical resonance frequency. This situation is of interest for the displacement measurements made with small and compact high-finesse cavities, where the radiation pressure effects are mainly due to the excitation of high-frequency internal acoustic modes of the mirrors [31, 35]. The susceptibility $\chi[\Omega]$ at frequency well below the mechanical resonance can be approximated as a real and positive expression [eq. (7)],

$$\chi[\Omega \ll \Omega_M] \simeq \chi[0] = \frac{1}{M\Omega_M^2}. \quad (35)$$

According to eq. (34), $\bar{\psi}$ has then to be negative in order to obtain an amplification factor $|\chi_{\text{eff}}/\chi|$ larger than 1. For any arbitrary negative value of the detuning $\bar{\psi}$, the condition $\zeta[0] = 1$ is reached for the value of the optomechanical parameter given by

$$\xi^2 = \frac{\xi_{\text{SQL}}^2[0]}{1 - \bar{\psi}/2\gamma}, \quad (36)$$

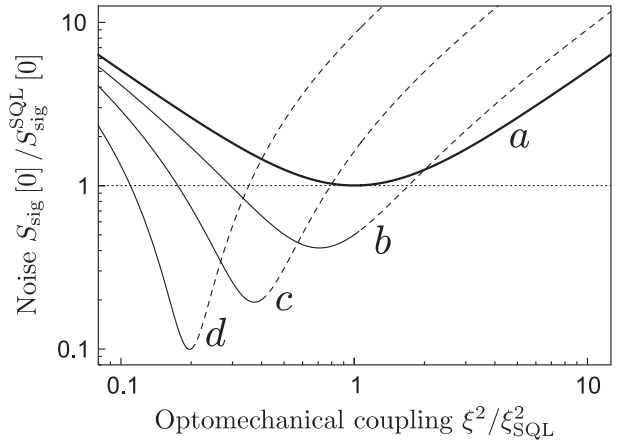


FIG. 2: Equivalent input noise S_{sig} at low frequency as a function of the optomechanical parameter ξ^2 , normalized to the SQL values ξ_{SQL}^2 and $S_{\text{sig}}^{\text{SQL}}$. Curves *a* to *d* are plotted for a normalized detuning $\bar{\psi}/\gamma$ equal to 0, -2 , -5 , and -10 , respectively. Dashed lines correspond to the unstable domain.

and the corresponding noise spectrum is equal to

$$\frac{S_{\text{sig}}[0]}{S_{\text{sig}}^{\text{SQL}}[0]} = \frac{1}{|\chi_{\text{eff}}[0]/\chi[0]|} = \frac{1}{1 - \bar{\psi}/2\gamma}. \quad (37)$$

It is then possible to arbitrarily reduce the equivalent input noise and to increase the sensitivity by choosing a large negative detuning. Note that although the optomechanical parameter ξ given by eq. (36) decreases as the noise spectrum, it corresponds to a larger incident intensity [see eq. (25)]. Increasing the sensitivity thus requires a larger input power.

Figure 2 shows the equivalent input noise $S_{\text{sig}}[0]$ as a function of the optomechanical parameter ξ , for different values of the detuning $\bar{\psi}$. Curve *a* is obtained at resonance ($\bar{\psi} = 0$). The noise reaches the standard quantum limit for $\xi = \xi_{\text{SQL}}$ and is larger than this limit elsewhere. Since ξ^2 is proportional to the incident intensity [eq. (25)], the additional noise for $\xi < \xi_{\text{SQL}}$ corresponds to the phase noise which is dominant at low intensity, whereas the additional noise for $\xi > \xi_{\text{SQL}}$ corresponds to the radiation pressure noise, dominant at high intensity. The behavior is similar for a detuned cavity (curves *b* to *d*), with a minimum noise reached at decreasing values of ξ as the detuning increases. The minimum noise is actually better than the one given by eq. (37). A more accurate optimization of the noise spectrum (30) leads to

$$\xi_{\text{min}}^2 = \frac{\xi_{\text{SQL}}^2[0]}{\sqrt{1 + (\bar{\psi}/2\gamma)^2}}, \quad (38)$$

$$\frac{S_{\text{sig}}^{\text{min}}[0]}{S_{\text{sig}}^{\text{SQL}}[0]} = \sqrt{1 + (\bar{\psi}/2\gamma)^2} + \bar{\psi}/2\gamma, \quad (39)$$

which tends to $\gamma/|\bar{\psi}|$ for large detunings. As an example, the curve *d* corresponding to a detuning $\bar{\psi} = -10\gamma$ exhibits a noise reduction by a factor 10. Finally note that

as the amplification by the mirror increases with the detuning, the optimum working point becomes nearer and nearer to the unstable domain shown as dashed curves in Fig. 2. It however always stays in the stable domain of the bistable behavior given by eq. (11).

VI. SENSITIVITY IMPROVEMENT AT HIGH FREQUENCY

We now study the sensitivity improvement at frequency larger than the mechanical resonance frequency. This situation corresponds for example to gravitational-wave interferometers where the main motion of the mirror is due to the pendular suspension which has very low resonance frequencies [1, 2]. In this case, the susceptibility $\chi[\Omega]$ can be approximated as a real but negative expression [eq. (7)],

$$\chi[\Omega \gg \Omega_M] \simeq -\frac{1}{M\Omega^2}, \quad (40)$$

so that the amplification factor $|\chi_{\text{eff}}/\chi|$ is now larger than 1 for a positive detuning $\bar{\psi}$. Since the susceptibility is frequency dependent, the condition $\zeta[\Omega] = 1$ can be satisfied at only one frequency. As a consequence, for a resonant cavity ($\bar{\psi} = 0$) and for a fixed optomechanical parameter ξ , the standard quantum limit is reached at a single frequency Ω_{SQL} given by eq. (31),

$$M\Omega_{\text{SQL}}^2 = |\chi[\Omega_{\text{SQL}}]|^{-1} = 2\hbar\xi^2. \quad (41)$$

Curve *a* of Fig. 3 shows the resulting noise spectrum at resonance, which reaches the standard quantum limit (dashed line) at frequency Ω_{SQL} . The radiation pressure noise is dominant at lower frequency with a $1/\Omega^4$ dependence, whereas the constant phase noise limits the sensitivity at higher frequency.

Curves *b* to *d* show the noise obtained for a detuned cavity with the same optomechanical parameter ξ . Although these curves exhibit a larger noise at low frequency than in the resonant case, one gets a significant noise reduction below the standard quantum limit in the intermediate frequency domain. The noise reduction becomes larger and larger as the detuning increases. An optimization of the noise spectrum (30) for a given detuning $\bar{\psi}$ and optomechanical parameter ξ leads to the optimal frequency Ω_{min} and noise spectrum $S_{\text{sig}}^{\text{min}}$,

$$\Omega_{\text{min}}^2 = \Omega_{\text{SQL}}^2 \sqrt{1 + (\bar{\psi}/2\gamma)^2}, \quad (42)$$

$$\frac{S_{\text{sig}}^{\text{min}}[\Omega_{\text{min}}]}{S_{\text{sig}}^{\text{SQL}}[\Omega_{\text{min}}]} = \sqrt{1 + (\bar{\psi}/2\gamma)^2} - \bar{\psi}/2\gamma. \quad (43)$$

The noise spectrum has an expression similar to eq. (39) obtained at low frequency, except for the sign of the detuning $\bar{\psi}$. As previously, the noise ratio (43) tends to $\gamma/\bar{\psi}$ for large detunings and one gets a noise reduction by a factor 10 for a detuning $\bar{\psi} = 10\gamma$.

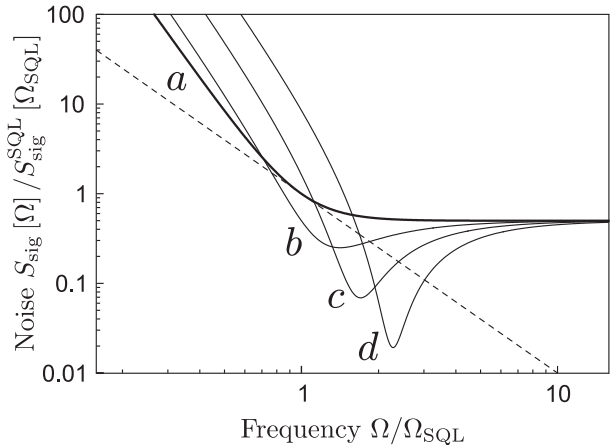


FIG. 3: Equivalent input noise $S_{\text{sig}}[\Omega]$ at high frequency as a function of frequency Ω , normalized to the SQL values Ω_{SQL} and $S_{\text{sig}}^{\text{SQL}}[\Omega_{\text{SQL}}]$. Curves *a* to *d* are plotted for the same optomechanical parameter ξ and for increasing normalized detunings $\bar{\psi}/\gamma$, equal to 0, 2, 5, and 10, respectively. Dashed line corresponds to the standard quantum limit.

VII. ULTIMATE QUANTUM LIMIT

The results of the previous sections seem to indicate that an arbitrarily large sensitivity improvement can be obtained both in the low and high frequency regimes since the equivalent input noise evolves in both cases as $\gamma/\bar{\psi}$ for large detunings. This actually is a consequence of the approximation made on the mechanical susceptibility which was assumed to have no imaginary part. It is possible to derive the optimal sensitivity improvement at a given frequency Ω without any assumption on the mechanical susceptibility $\chi[\Omega]$. An optimization of the noise spectrum (30) with respect to the optomechanical parameter ξ leads to,

$$\xi_{\text{min}}^2 = \frac{\xi_{\text{SQL}}^2[\Omega]}{\sqrt{1 + (\bar{\psi}/2\gamma)^2}}, \quad (44)$$

$$\frac{S_{\text{sig}}^{\text{min}}[\Omega]}{S_{\text{sig}}^{\text{SQL}}[\Omega]} = \sqrt{1 + (\bar{\psi}/2\gamma)^2} + \frac{\bar{\psi}}{2\gamma} \frac{\text{Re}(\chi[\Omega])}{|\chi[\Omega]|}, \quad (45)$$

where $\xi_{\text{SQL}}[\Omega]$ is the optomechanical parameter for which the standard quantum limit is reached at frequency Ω for a resonant cavity [eq. (32)]. As compared to eqs. (38) and (39) obtained at low frequency and for a real mechanical susceptibility, the only difference is the last term in eq. (45) which has a smaller amplitude when the susceptibility has a non-zero imaginary part. As a consequence, the equivalent input noise no longer decreases as $\gamma/\bar{\psi}$ for very large detunings, and it reaches a non-zero minimum value at a finite detuning given by,

$$\bar{\psi}_{\text{min}}/2\gamma = -\frac{\text{Re}(\chi[\Omega])}{|\text{Im}(\chi[\Omega])|}, \quad (46)$$

$$S_{\text{sig}}^{\text{min}}[\Omega] = \hbar |\text{Im}(\chi[\Omega])|. \quad (47)$$

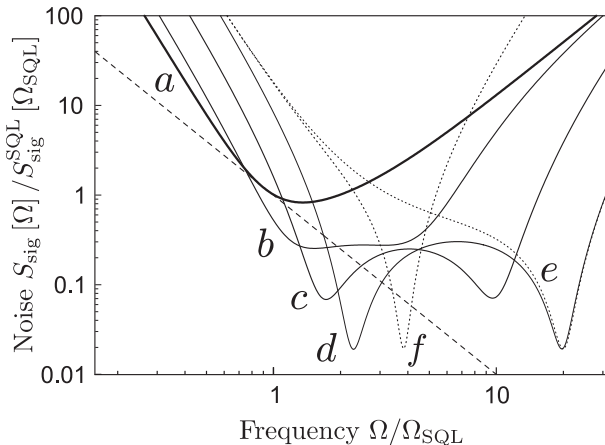


FIG. 4: Equivalent input noise $S_{\text{sig}}[\Omega]$ at high frequency as a function of frequency Ω , normalized to the SQL values Ω_{SQL} and $S_{\text{sig}}^{\text{SQL}}[\Omega_{\text{SQL}}]$. All curves are plotted for the same optomechanical parameter ξ , and for the same finite cavity bandwidth $\Omega_{\text{cav}} = 2\Omega_{\text{SQL}}$, except curve f for which $\Omega_{\text{cav}} = \Omega_{\text{SQL}}/3$. Curves a to d correspond to positive normalized detunings $\bar{\psi}/\gamma$ equal to 0, 2, 5, and 10, respectively. Curves e and f are obtained for a negative normalized detuning of -10 . The dashed line is the standard quantum limit.

One then gets a limit to the sensitivity improvement which is only related to the dissipation mechanism of the mechanical motion, via the imaginary part of the susceptibility. This is nothing but the ultimate quantum limit already predicted in the case of interferometric measurements with squeezed-state injection [5]. The same ultimate limit is thus reached by cavity detuning.

VIII. CAVITY WITH A FINITE BANDWIDTH

We finally study the effect of a finite cavity bandwidth $\Omega_{\text{cav}} = \gamma/\tau$. The optical equations in the case of a detuned cavity with a finite bandwidth are much more complex than the ones given in the previous sections. As an example, the input-output relation for the phase quadrature is derived from eqs. (12), (16) and (17),

$$q^{\text{out}}[\Omega] = 2\xi \frac{\gamma^2 + \bar{\psi}^2 - i\gamma\Omega\tau}{\Delta} (X_m[\Omega] + X_{\text{sig}}[\Omega]) + \frac{1}{\Delta} \left(\gamma^2 + \bar{\psi}^2 + \Omega^2\tau^2 \frac{\gamma^2 - \bar{\psi}^2}{\gamma^2 + \bar{\psi}^2} \right) q^{\text{in}}[\Omega] - \frac{2}{\Delta} \Omega^2\tau^2 \frac{\gamma\bar{\psi}}{\gamma^2 + \bar{\psi}^2} p^{\text{in}}[\Omega], \quad (48)$$

and can be compared to the simpler relation (24) obtained in the case of an infinite cavity bandwidth. We have computed the equivalent input noise S_{sig} from the previous input-output relation and from eqs. (13) to (15), by using the formal language Mathematica. Figure 4 shows the resulting noise obtained at high frequency,

that is for a mechanical susceptibility approximated by the real and negative expression (40). All curves are plotted for the same optomechanical parameter ξ and, except for curve f , with a cavity bandwidth Ω_{cav} equal to $2\Omega_{\text{SQL}}$, where Ω_{SQL} is related to ξ by eq. (41).

Curve a of Fig. 4 shows the equivalent input noise at resonance ($\bar{\psi} = 0$). As compared to a cavity with an infinite bandwidth (curve a of Fig. 3), the noise is no longer constant at high frequency but increases with the frequency. This is a consequence of the low-pass filtering of the signal by the cavity for frequencies larger than the cavity bandwidth. Curves b to d show the equivalent noise spectrum obtained for positive and increasing detunings. One clearly observes two resonant dips with a structure very similar to the one already predicted for signal-recycled gravitational-wave interferometers [12]. These two resonances become deeper and more separated as the detuning increases.

The dip at the lowest frequency is very similar to the one obtained for an infinite cavity bandwidth, as well in frequency position, in width, and in noise reduction (compare curves b to d of Figs. 3 and 4). In both cases, the dip can be associated with the resonance of the amplification factor $|\chi_{\text{eff}}/\chi|$. From eq. (20), one indeed finds that the effective susceptibility χ_{eff} has a Lorentzian shape with a resonance frequency Ω_- very close to the dip position Ω_{min} [eq. (42)] and given for a large detuning by,

$$\Omega_- \simeq \Omega_{\text{SQL}} \sqrt{\frac{\bar{\psi}}{2\gamma}}. \quad (49)$$

Taking a finite cavity bandwidth thus changes the width of the effective mechanical resonance, as already discussed in section III [see eq. (21)], but it has no apparent effect on the sensitivity improvement around the resonance frequency Ω_- .

The second dip only exists for a finite cavity bandwidth and is a consequence of the optical dynamics in the cavity. Its frequency actually corresponds to the resonance frequency Ω_+ of the term $1/\Delta$ which appears both in the input-output relation (48) and in the radiation pressure forces (13) to (15),

$$\Omega_+ = \Omega_{\text{cav}} \sqrt{1 + \frac{\bar{\psi}^2}{\gamma^2}}. \quad (50)$$

In contrast to the first dip for which the signal amplification is only obtained with a positive detuning, the second dip exists both for positive and negative detunings. This is clearly visible in Fig. 4 where curves d and e are plotted for the same parameters but for reverse detunings. Note however that the stability conditions are very different in the two situations. In particular the dynamic stability condition (22) is always satisfied for a negative detuning whereas it is very restrictive for a positive detuning. Curves b to d of Fig. 4 are actually unstable for a reasonably not too large mechanical damping Γ .

The sensitivity improvement at the resonance frequencies Ω_{\pm} can be computed from the analytic expression given by Mathematica. One gets for a large detuning $\overline{\psi}$,

$$\frac{S_{\text{sig}}[\Omega_{\pm}]}{S_{\text{sig}}^{\text{SQL}}[\Omega_{\text{SQL}}]} \simeq \frac{2\gamma^2}{\overline{\psi}^2}. \quad (51)$$

The two dips have thus the same depth, as it can be observed in Fig. 4. In this expression, the noise is normalized to the standard quantum limit at frequency Ω_{SQL} . It is also of interest to compute the noise reduction below the standard quantum limit, that is the ratio between the noise at frequency Ω_{\pm} and the standard quantum limit (33) at the same frequency,

$$\frac{S_{\text{sig}}[\Omega_{\pm}]}{S_{\text{sig}}^{\text{SQL}}[\Omega_{\pm}]} \simeq \frac{2\gamma^2}{\overline{\psi}^2} \left(\frac{\Omega_{\pm}}{\Omega_{\text{SQL}}} \right)^2. \quad (52)$$

From eq. (49), the ratio tends to $\gamma/\overline{\psi}$ at the resonance frequency Ω_- of the first dip. This result is identical to the one obtained in section VI for an infinite cavity bandwidth. At the resonance frequency Ω_+ of the second dip [eq. (50)], the noise ratio (52) is equal to $2(\Omega_{\text{cav}}/\Omega_{\text{SQL}})^2$. The noise is then reduced below the standard quantum limit only if the cavity bandwidth is small enough, as shown by curves *e* and *f* in Fig. 4, respectively obtained for $\Omega_{\text{cav}} = 2\Omega_{\text{SQL}}$ and $\Omega_{\text{cav}} = \Omega_{\text{SQL}}/3$.

Finally note that eq. (51) seems to indicate that an arbitrarily small equivalent input noise can be reached by increasing the detuning. As for an infinite cavity bandwidth (section VII), it can be shown that the noise is always larger than the ultimate quantum limit (47), which can be reached at every frequency Ω by an appropriate choice of the parameters ξ , ψ , and Ω_{cav} .

IX. CONCLUSION

We have studied the quantum limits of an optomechanical sensor based on a detuned high-finesse cavity with a movable mirror. We have shown that the sensitivity to a variation of the cavity length can be improved beyond the standard quantum limit, up to the ultimate quantum limit which only depends on the dissipation mechanisms of the mirror motion. This improvement is due to an amplification of the signal by the mirror displacements. The coupling between the mirror motion and the intracavity light field actually changes the dynamics of the mirror, both via its spring constant and its damping. But the mirror motion also becomes sensitive to the signal and can amplify the effect of the signal on the intracavity field. For a finite cavity bandwidth, one gets a sensitivity improvement very similar to the one predicted in signal-recycled gravitational-waves interferometers, with two dips in the equivalent input noise which are related to the effective mechanical resonance of the mirror and to the optical dynamics in the cavity. A high-finesse cavity with a movable mirror thus appears as a model system to test quantum effects in large-scale interferometers.

Acknowledgments

We thank Jean-Michel Courty and Julien Le Bars for fruitful discussions. This work was partially funded by EGO (collaboration convention EGO-DIR-150/2003 for a study of quantum noises in gravitational waves interferometers).

-
- [1] C. Bradaschia *et al*, Nucl. Instrum. Methods Phys. Res. A **289**, 518 (1990)
 - [2] A. Abramovici *et al*, Science **256**, 325 (1992)
 - [3] P. Fritschel, Proc. SPIE **4856**, 282 (2002)
 - [4] C.M. Caves, Phys. Rev. D **23**, 1693 (1981)
 - [5] M.T. Jaekel and S. Reynaud, Europhys. Lett. **13**, 301 (1990)
 - [6] V.B. Braginsky and F. Ya Khalili, Quantum Measurement (Cambridge University Press, Cambridge, 1992)
 - [7] M. Xiao, L.A. Wu and H.J. Kimble, Phys. Rev. Lett. **59**, 278 (1987)
 - [8] P. Grangier, R.E. Slusher, B. Yurke and A. LaPorta, Phys. Rev. Lett. **59**, 2153 (1987)
 - [9] K. McKenzie, D.A. Shaddock, D.E. McClelland, B.C. Buchler and P.K. Lam, Phys. Rev. Lett. **88**, 231102 (2002)
 - [10] H.J. Kimble, Y. Levin, A.B. Matsko, K.S. Thorne and S.P. Vyatchanin, Phys. Rev. D **65**, 022002 (2002)
 - [11] J.M. Courty, A. Heidmann and M. Pinard, Phys. Rev. Lett. **90**, 083601 (2003)
 - [12] A. Buonanno and Y. Chen, Phys. Rev. D **64**, 042006 (2001)
 - [13] J. Harms, Y. Chen, S. Chelkowski, A. Franzen, H. Vahlbruch, K. Danzmann and R. Schnabel, Phys. Rev. D **68**, 042001 (2003)
 - [14] C. Fabre, M. Pinard, S. Bourzeix, A. Heidmann, E. Giacobino and S. Reynaud, Phys. Rev. A **49**, 1337 (1994)
 - [15] S. Mancini and P. Tombesi, Phys. Rev. A **49**, 4055 (1994)
 - [16] S. Bose, K. Jacobs and P.L. Knight, Phys. Rev. A **59**, 3204 (1999)
 - [17] S. Mancini, V. Giovannetti, D. Vitali and P. Tombesi, Phys. Rev. Lett. **88**, 120401 (2002)
 - [18] M. Pinard, A. Dantan, D. Vitali, O. Arcizet, T. Briant and A. Heidmann, Europhys. Lett. **72**, 747 (2005)
 - [19] A. Heidmann, Y. Hadjar and M. Pinard, App. Phys. B **64**, 173 (1997)
 - [20] Y. Hadjar, P.F. Cohadon, C.G. Aminoff, M. Pinard and A. Heidmann, Europhys. Lett. **47**, 545 (1999)
 - [21] P.F. Cohadon, A. Heidmann and M. Pinard, Phys. Rev. Lett. **83**, 3174 (1999)
 - [22] I. Tittonen *et al.*, Phys. Rev. A **59**, 1038 (1999)
 - [23] A. Buonanno and Y. Chen, Phys. Rev. D **65**, 042001 (2002)
 - [24] V.B. Braginsky and F.Ya. Khalili, Phys. Lett. A **257**,

- 241 (1999)
- [25] V.B. Braginsky, F.Ya. Khalili and P.S. Volikov, *Phys. Lett. A* **287**, 31 (2001)
- [26] B.S. Sheard, M.B. Gray, C.M. Mow-Lowry, D.E. McClelland and S.E. Whitcomb, *Phys. Rev. A* **69**, 051801(R) (2004)
- [27] V.B. Braginsky and S.P. Vyatchanin, *Phys. Lett. A* **293**, 228 (2002)
- [28] S.W. Schediwy, C. Zhao, L. Ju and D.G. Blair, *Class. Quantum Grav.* **21**, S1253 (2004)
- [29] L. Landau and E. Lifshitz, *Course of Theoretical Physics: Statistical Physics* (Pergamon, New York, 1958), Chap. 12
- [30] A. Dorsel, J.D. McCullen, P. Meystre, E. Vignes and H. Walther, *Phys. Rev. Lett.* **51**, 1550 (1983)
- [31] M. Pinard, P.F. Cohadon, T. Briant and A. Heidmann, *Phys. Rev. A* **63**, 013808 (2000)
- [32] J.M. Courty, A. Heidmann and M. Pinard, *Eur. Phys. J. D* **17**, 399 (2001)
- [33] C.H. Metzger and K. Karrai, *Nature* **432**, 1002 (2004)
- [34] H. Haken, in *Encyclopedia of Physics XXV/2c*, edited by S. Flugge (Springer-Verlag, Heidelberg, 1970)
- [35] T. Briant, P.F. Cohadon, A. Heidmann and M. Pinard, *Phys. Rev. A* **68**, 033823 (2003)